

# On the plasticity of small-scale nickel–titanium shape memory alloys

Carl P. Frick,<sup>a,\*</sup> Blythe G. Clark,<sup>b,c,1</sup> Andreas S. Schneider,<sup>b</sup> Robert Maaß,<sup>d</sup>  
Steven Van Petegem<sup>d</sup> and Helena Van Swygenhoven<sup>d</sup>

<sup>a</sup>University of Wyoming, Department of Mechanical Engineering, Laramie, WY 82071, USA

<sup>b</sup>Max Planck Institute for Metals Research, Heisenbergstrasse 3, 70569 Stuttgart, Germany

<sup>c</sup>INM-Leibniz Institute for New Materials, Campus Building D2 2, 66123 Saarbrücken, Germany

<sup>d</sup>Paul Scherrer Institute, CH-5232 Villigen, Switzerland

Received 8 December 2009; accepted 10 December 2009

Available online 16 December 2009

Focused ion beam machined compression pillars created from [1 1 1], [0 0 1] and [2 1 0] NiTi demonstrate that orientation plays a dominant role in determining dislocation flow stress in stress-induced martensite. This is in contrast to bulk NiTi in which martensite strength is primarily dictated by precipitate size. Post-mortem transmission electron microscopy and Laue microdiffraction measurements reveal respectively dense dislocation structures and stabilized martensite consistent with bulk observations in heavily deformed NiTi.

Published by Elsevier Ltd. on behalf of Acta Materialia Inc.

**Keywords:** Plastic deformation; Shape memory alloys (SMA); Compression test; Transmission electron microscopy (TEM); Micropillars

Nickel–titanium (NiTi) is of particular interest because of its unique strain recovery behavior. Under the appropriate conditions, NiTi is capable of recovering up to approximately 8% strain upon removal of the applied load (i.e. pseudoelasticity) or upon the application of heat (i.e. shape memory behavior) [1,2]. Essentially, NiTi experiences a thermoelastic, stress-induced martensitic phase transformation, whereby the original crystal lattice experiences a shear-like phase transformation that is reversible.

Widespread use of NiTi is limited because mechanical behavior is extremely sensitive to composition, microstructure and processing history. For example, applied strain recovery associated with the martensitic phase transformation for various microstructures degrades significantly before 16 cycles [3], and high-cycle fatigue shows relatively low fracture toughness values [4]. It has been theorized that an increased propensity for defect nucleation exists at the austenite–martensite interface, which hinders phase transformation recovery [3]. However, martensitic stabilization associated with cold

working of NiTi has also proven to be useful by generating a two-way shape memory effect; when processed correctly, dislocations can be used to direct the formation of the martensite variants, allowing a spontaneous shape recovery under thermal cycling in the absence of applied stress [5]. While dislocations are well known to influence or inhibit the martensitic phase transformation in NiTi, the fundamental relationship between the two is not well understood.

In order to gain deeper insight into the mechanisms associated with NiTi plastic deformation, the effect of size scale on the compressive flow stress of stress-induced martensite is investigated in this study. Focused ion beam (FIB) machined compression pillars created from aged [1 1 1], [0 0 1] and [2 1 0] Ti–50.9 at.% Ni single crystals, as well as pillars cut from individual grains in solutionized polycrystalline NiTi were tested. For the NiTi used in this study, the austenite parent phase (B2) is stable at room temperature, and the martensite phase (B19') is induced upon loading [6,7].

However, to better understand the mechanisms involved, additional microstructural analysis was first performed on previously deformed samples. In a prior study by the current authors, martensite flow stress values in aged [1 1 1] NiTi compression pillars ranging in diameter from 2 μm to 200 nm were shown to be unaffected by pil-

\*Corresponding author. Tel.: +1 (307) 766 4068; e-mail: [cfrick@uwyo.edu](mailto:cfrick@uwyo.edu)

<sup>1</sup>Present address: Sandia National Laboratories, Albuquerque, NM 87185, USA.

lar size [7]. This was partly expected due to randomly distributed, semicoherent  $\text{Ti}_3\text{Ni}_4$  precipitates 10 nm in diameter, with interparticle spacing of the same order. Because the precipitate spacing was significantly smaller than the smallest diameter tested (below 200 nm), these precipitates probably dominated the stress needed for dislocation motion. However, despite the known influence of these precipitates, preliminary testing of a 1  $\mu\text{m}$  diameter [2 1 0] NiTi pillar surprisingly demonstrated a reduced martensite flow stress at approximately one-third the average value of the [1 1 1] from [7]. This observed orientation dependence is in stark contrast with bulk [8] and micro/nanoindentation NiTi studies [9,10], which show that precipitate size and coherency strongly influence martensite flow stress and dominate over single-crystal orientation.

Figure 1 displays the stress–strain behavior and a scanning electron microscope (SEM) image of a heavily deformed [1 1 1] NiTi pillar approximately 2  $\mu\text{m}$  in diameter. The initial loading/unloading cycles of the pillar at low strains (<6%) demonstrate pseudoelasticity, as evidenced by the flag-shaped hysteresis loops in the stress–strain graph (Fig. 1a). This is a signature of the recoverable austenite-to-martensite phase transformation, which dominates deformation at low strains. Upon further loading the pillar transforms to martensite, which proceeds to deform primarily elastically until the curve exhibits a large burst in displacement at a stress of approximately 3000 MPa. Such bursts have been demonstrated in other load-controlled micropillar studies, and have been shown to correlate to dislocation events [11,12]. Because the focus of this study is the martensite plastic deformation, only pillars taken to high strains (>10%) were investigated. SEM imaging of the

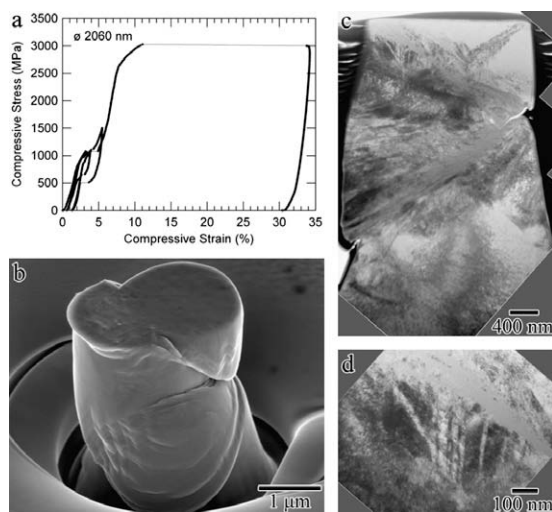


**Figure 1.** Compression behavior and electron microscopy images of a heavily deformed [1 1 1] NiTi pillar approximately 2  $\mu\text{m}$  in diameter taken from a previous study [7]. (a) Stress–strain curve demonstrating pseudoelasticity in the first two loading cycles, and upon further loading a large burst in displacement at a stress of approximately 3000 MPa, after which the strain is not recovered. (b) SEM image showing massive slip primarily along three slip planes. (c) Bright-field TEM micrographs of a cross-sectional sample overlapped together to display the entire pillar. (d) Higher-magnification TEM image taken from the upper left corner of the pillar. TEM images show distinct slip traces and pockets of twins, believed to be residual martensite.

pillar (Fig. 1b) shows massive slip deformation, which is representative of all pillars tested to large strains. Interestingly, saw-tooth features are also observed on the surface. Such triangular features were infrequently observed, and are probably caused by the stabilized martensite variants formed during the phase transformation, previously observed in NiTi samples [13].

Post-deformation, the pillar shown in Figure 1b was sectioned via FIB into a transmission electron microscopy (TEM) sample, in a manner similar to that outlined in Frick et al. [12]. Figure 1c shows bright-field TEM micrographs overlapped together to display the entire pillar, while Figure 1d shows a higher-magnification image of the upper left pillar corner. Both Figure 1c and d illustrate distinct slip traces and pockets of twins, believed to be residual martensite. Although the phase transformation is pseudoelastic, dislocation-assisted stabilized martensite is often observed in heavily deformed NiTi [10]. Compression-induced martensite is known to take the form of two twin-related martensite plates, formally termed correspondence variant pairs (CVPs) [14,15]. From Figure 1d, the width of the CVPs range from approximately 15 to 30 nm. Additionally, Figure 1c and d show dense dislocation tangles throughout the pillar. These results are not expected to significantly vary over the size scales tested in this study, as near 200 nm diameter NiTi pillars compressed to approximately 20% strain during in situ TEM testing also demonstrated residual dislocations and stabilized martensite [16]. It is important to note that Figure 1b and c also demonstrate large slip traces through the entire pillar diameter, between 30° and 40° relative to the applied load. Therefore, although the dispersed  $\text{Ti}_3\text{Ni}_4$  precipitates and CVP martensite structure heavily influence dislocation motion, once the flow stress was reached, dislocations propagated across the width of the sample.

Similar results shown in Figure 2 were obtained for a 2.8  $\mu\text{m}$  diameter NiTi pillar tested by Laue microdiffraction at the MicroXAS beam line of the Swiss Light Source [17]. This sample was cut from the same parent crystal as the previous example in Figure 1, and therefore has the same nominal composition and precipitate microstructure. The [2 1 0] orientation was chosen because preliminary results demonstrated a much lower martensitic flow stress than that observed in [1 1 1] NiTi [7]. Discrete spatial diffraction measurements along the pillar length before testing (Fig. 2a) and after testing (Fig. 2b) demonstrate the presence of austenite phase throughout. However, after compression, the upper one-fifth of the pillar revealed the presence of the martensite phase (Fig. 2c). Thus, Laue diffraction measurements of [2 1 0] NiTi coincide with TEM imaging of [1 1 1] NiTi, demonstrating stabilized stress-induced martensite. It is important to note that due to pillar taper, stress values will nominally depend on spatial location along the length of the pillar [12], being largest at the top. Using the diameter at the pillar top, the maximum stress measured during compression was approximately 900 MPa, approximately one-third the average flow stress value observed for the [1 1 1] NiTi pillars [7]. Figure 2d and e display the (022)-peak of the austenite phase before and after testing, respectively. Before testing a mild anisotropic broad-

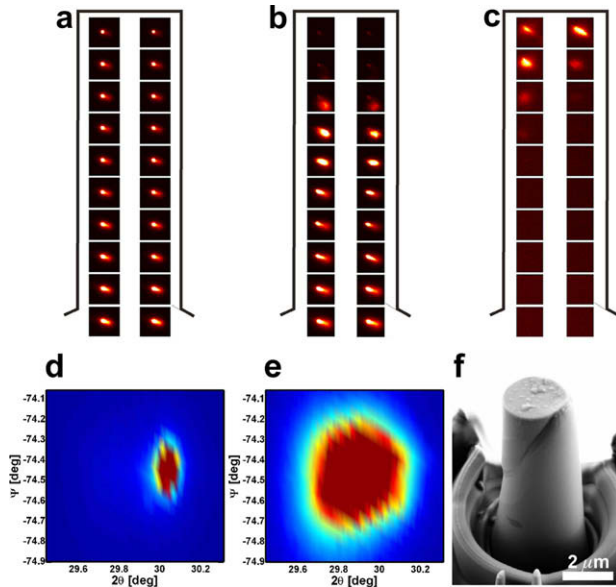


**Figure 2.** Spatially resolved Laue diffraction maps for a [2 1 0] NiTi pillar (a) before deformation showing the (02 $\bar{2}$ ) austenite peak throughout the pillar, and (b) after deformation revealing that the austenite is strongly reduced in the upper pillar post-deformation. (c) A diffraction peak corresponding to residual stabilized martensite appears post-deformation, observed near the top of the pillar. A blow-up of the (02 $\bar{2}$ ) austenite diffraction peak taken at the center of the pillars before and after deformation is shown in (d) and (e), respectively.  $\Psi$  and  $2\theta$  describe the azimuthal and radial angle, respectively. (f) SEM micrograph of the pillar post-compression illustrating significant slip on preferential slip planes.

ening is observed, possibly due to the presence of the semicoherent  $\text{Ti}_3\text{Ni}_4$  precipitates and/or the sample preparation technique. After deformation the diffraction peaks are strongly broadened, both symmetrically and asymmetrically, or even split, depending on the probing position. SEM imaging of the pillar post-deformation shown in Figure 2f reveals heavy localized slip. These observations are qualitatively in agreement with Figure 1, indicating a pronounced heterogeneous microstructure with an increase in dislocation density and the presence of angular misorientations.

In order to further investigate the effect of orientation on martensite plasticity of small-scale NiTi, several compression pillars with crystal orientations of [1 1 1], [0 0 1] and [2 1 0] were tested. All compression samples were taken from a previous study, which focused on the pseudoelastic response rather than martensitic plasticity [6]. An important finding from the previous study is that pseudoelasticity becomes inhibited for diameters below 400 nm, and fully inhibited for diameters below 200 nm. However, in situ TEM investigations [16] for similar sized specimens reveal that at low strains a recoverable martensitic transformation does occur, and at high strains recovery becomes inhibited, probably due to dislocation-stabilized martensite. Therefore it is believed that the martensitic transformation occurs for all samples shown here, regardless of diameter.

All single-crystal samples were cut from the same parent specimen (Ti–50.9 at.% Ni), and each was given a heat treatment of 350 °C for 1.5 h to induce randomly

distributed, semicoherent  $\text{Ti}_3\text{Ni}_4$  precipitates approximately 10 nm in diameter. In the case of bulk single-crystal NiTi, the precipitate structure has clearly been shown to have a dominating effect on the martensite flow stress [8]. Thus, to gauge the influence of precipitates on the mechanical behavior at small scales, additional pillars were cut from bulk polycrystalline NiTi heat treated at 600 °C for 1.5 h and immediately water quenched. Previous studies with polycrystalline NiTi of the same composition and given identical heat treatment illustrate a virtually solutionized microstructure (i.e.  $\text{Ti}_3\text{Ni}_4$  precipitates are less than 1 nm in size) [10]. Because grains in the polycrystalline NiTi are 70  $\mu\text{m}$  in diameter on average, it was possible to cut single-orientation pillars within individual grains. Electron backscatter diffraction was utilized to measure the crystal orientation of each grain.

It is important to note that for isothermal testing, due to the directional nature of the martensitic phase transformation, the transformation will proceed on the most favorably oriented CVP. This behavior is analogous to the Schmid law in conventional elastic–plastic materials, which relates the applied stress to the resolved shear stress needed for dislocation motion. In a comparable fashion, a resolved shear stress factor ( $\text{RSSF}_M$ ) for the formation of the most favorable martensite CVP can be calculated using previously determined martensite crystallographic data [18]. For the orientations tested in this study in compression, the  $\text{RSSF}_M$  values for the [1 1 1], [0 0 1] and [2 1 0] orientations are 0.24, 0.37 and 0.50, respectively. A low  $\text{RSSF}_M$  means that the phase transformation is not favored, and a higher stress is needed to initiate and propagate the martensitic phase transformation, relative to a high  $\text{RSSF}_M$ . It is acknowledged that these transformation parameters are not strictly valid for NiTi with finely distributed, semicoherent precipitates [19]. The local coherency stress fields caused by the precipitates will act as nucleation sites for the martensite, while inhibiting plastic flow [20,21]. Additionally, it is important to note that for bulk crystals, there is sufficient volume of material to sample multiple variants to achieve a volume–average response. TEM measurements shown in Figure 1d illustrate martensite variants approximately 15–30 nm in width. Therefore it is acknowledged that for the pillars tested in this study, with diameters ranging from approximately 200 nm to 2  $\mu\text{m}$ , the “volume–average” assumption may fall into question.

Figure 3 shows two graphs using the stress value at 10% strain for all orientations and microstructures tested. This strain amount was chosen because it is beyond the theoretical compressive transformation strain for any of the tested orientations [8], and all pillars loaded beyond 10% strain exhibited visual deformation in SEM images, as well as significant irrecoverable stress–strain deformation. Figure 3a plots these martensitic flow stress values as a function of pillar diameter. Flow stress of the [1 1 1] and [0 0 1] NiTi pillars showed no significant correlation with diameter, while the [2 1 0] and solutionized pillars exhibited a weak relationship ( $\sigma_{10\%} \propto d^{-0.23}$ ) relative to conventional face-centered cubic metals ( $\sigma_y \propto d^{-0.6} - d^{-1.0}$ ) [12,22,23]. Flow stress values for solutionized pillars vary significantly

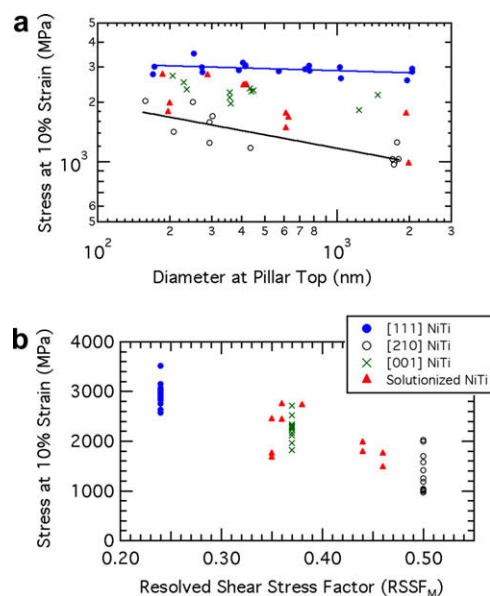


**Figure 3.** Stress values at 10% strain plotted as a function of (a) pillar diameter and (b) resolved shear stress factor for all samples tested. The [1 1 1] NiTi (taken from Ref. [7]) and [0 0 1] NiTi pillars exhibit no correlation between flow stress and pillar diameter, while [2 1 0] demonstrates a slight correlation (stress related to  $d^{-0.2}$ ). Solutionized NiTi pillars cut from individual grains in polycrystalline NiTi exhibited a wide range of values.

within the observed range, and no well-defined connection to diameter was observed.

However, measured flow stresses did correlate well with the orientation dependence of the stress-induced martensitic phase transformation, shown in Figure 3b. For example, the average and standard deviation of the flow stresses for the [2 1 0], [0 0 1] and the [1 1 1] pillars were  $1410 \pm 388$ ,  $2322 \pm 303$  and  $2939 \pm 206$  MPa, respectively. Although significant scatter exists, the disparity of strength values between the orientations strongly indicates that the orientation has a pronounced influence on the martensite flow stress. This phenomenon is not observed in bulk samples of similar microstructure where martensitic flow stresses between 2000 and 2100 MPa are observed regardless of orientation for peak-aged bulk single-crystal NiTi [8].

It is important to note that although Figure 3b demonstrates that the stress needed to initiate/propagate martensite and the martensite flow stress are strongly correlated, post-mortem TEM and Laue diffraction analysis are inherently limited when describing the kinetics of both the martensite and dislocation behavior. Therefore the precise governing mechanism explaining this observation remains ambiguous.

The strong relationship between orientation and martensite flow stress irrespective of precipitate structure indicates an extremely unique finding for small-scale NiTi. TEM images (Fig. 1c and d) demonstrate stabilized martensite CVPs approximately 15–30 nm in width alongside dense dislocation structures, indicating that the progression of dislocation motion and martensite formation is complex and probably interwoven, as suggested by previous studies [3,24]. This observation is complemented by the Laue diffraction measurements

(Fig. 2) that also show residual martensite in combination with plasticity. Further in situ TEM investigation is needed to provide insight into the microstructural deformation evolution in nanoscale NiTi pillars.

The authors acknowledge the assistance of Ulrike Eigenthaler and Dr. Michael Hirscher with the DualBeam™ FIB, Birgit Heiland for assistance in TEM sample preparation, and Petra Sonnweber-Ribic for EBSD measurements. Additionally we thank Dr. Yuri Chumlyakov of the Siberian Physical Technical Institute for creating the single-crystal NiTi samples, as well as Dr. D. Grolimund and Dr. C.N. Borca at the Swiss Light Source whose outstanding efforts have made the microdiffraction experiments possible.

- [1] J.A. Shaw, S. Kyriakides, *J. Mech. Phys. Solids* 43 (1995) 1243.
- [2] K. Otsuka, X. Ren, *Prog. Mater. Sci.* 50 (2005) 511.
- [3] K. Gall, H. Maier, *Acta Mater.* 50 (2002) 4643.
- [4] A.L. Mckelvey, R.O. Ritchie, *J. Biomed. Mater. Res.* 47 (1999) 301.
- [5] P.Y. Manach, D. Favier, *Scr. Metall. Mater.* 28 (1993) 1417.
- [6] C.P. Frick, B.G. Clark, S. Orso, P. Sonnweber-Ribic, E. Arzt, *Scr. Mater.* 59 (2008) 7.
- [7] C.P. Frick, S. Orso, E. Arzt, *Acta Mater.* 55 (2007) 3845.
- [8] H. Sehitoglu, I. Karaman, R. Anderson, X. Zhang, K. Gall, H.J. Maier, Y. Chumlyakov, *Acta Mater.* 49 (2001) 747.
- [9] C.P. Frick, T.W. Lang, K. Spark, K. Gall, *Acta Mater.* 54 (2006) 2223.
- [10] C.P. Frick, A.M. Ortega, J. Tyber, A.E.M. Maksoud, H.J. Maier, Y.N. Liu, K. Gall, *Mater. Sci. Eng. A: Struct. Mater. Prop. Microstruct. Process.* 405 (2005) 34.
- [11] M.D. Uchic, D.M. Dimiduk, J.N. Florando, W.D. Nix, *Science* 305 (2004) 986.
- [12] C.P. Frick, B.G. Clark, S. Orso, A.S. Schneider, E. Arzt, *Mater. Sci. Eng. A: Struct. Mater. Prop. Microstruct. Process.* 489 (2008) 319.
- [13] L.C. Brinson, I. Schmidt, R. Lammering, *J. Mech. Phys. Solids* 52 (2004) 1549.
- [14] T.E. Buchheit, J.A. Wert, *Metall. Mater. Trans. A: Phys. Metall. Mater. Sci.* 27 (1996) 269.
- [15] K. Gall, H. Sehitoglu, *Int. J. Plast.* 15 (1999) 69.
- [16] J. Ye, R.K. Mishra, A.R. Pelton, A.M. Minor, *Acta Mater.* 58 (2010) 490.
- [17] R. Maass, S. Van Petegem, H. Van Swygenhoven, P.M. Derlet, C.A. Volkert, D. Grolimund, *Phys. Rev. Lett.* 99 (2007) 145505.
- [18] O. Matsumoto, S. Miyazaki, K. Otsuka, H. Tamura, *Acta Metall.* 35 (1987) 2137.
- [19] S. Miyazaki, S. Kimura, K. Otsuka, Y. Suzuki, *Scr. Metall.* 18 (1984) 883.
- [20] K. Gall, H. Sehitoglu, Y.I. Chumlyakov, I.V. Kireeva, H.J. Maier, *J. Eng. Mater. Technol. – Trans. ASME* 121 (1999) 28.
- [21] K. Gall, H. Sehitoglu, Y.I. Chumlyakov, I.V. Kireeva, H.J. Maier, *J. Eng. Mater. Technol. – Trans. ASME* 121 (1999) 19.
- [22] J.R. Greer, W.D. Nix, *Phys. Rev. B* 73 (2006).
- [23] C.A. Volkert, E.T. Lilleodden, *Philos. Mag.* 86 (2006) 5567.
- [24] D.M. Norfleet, P.M. Sarosi, S. Manchiraju, M.F.X. Wagner, M.D. Uchic, P.M. Anderson, M.J. Mills, *Acta Mater.* 57 (2009) 3549.